

# SANS Analysis of the Molecular Order in Poly( $\gamma$ -benzyl L-glutamate)/Deuterated Dimethylformamide (PBLG/d-DMF) under Shear and during Relaxation

Lynn M. Walker and Norman J. Wagner\*

Colburn Laboratory, Department of Chemical Engineering, University of Delaware, Newark, Delaware 19716

Received August 3, 1995; Revised Manuscript Received December 13, 1995<sup>§</sup>

**ABSTRACT:** Small-angle neutron scattering (SANS) has been used to measure the overall molecular alignment in solutions of PBLG/d-DMF during and after cessation of steady shear flow. A new technique for resolving order parameters from two-dimensional SANS data is presented. Results of this analysis show that during the period of time after cessation of flow from the linear regime, the overall molecular alignment in the velocity–vorticity projection increases, confirming previous birefringence measurements.

## Introduction

Liquid crystal polymers (LCPs) exhibit a complicated microstructural hierarchy which is coupled to applied flow fields. One physical picture which captures much of the observed rheological behavior is that of a polydomain fluid, where the nematic fluid exists over regions on the order of microns in length (domains) bounded by defects (or texture). Polydomain models predict scaling with strain during flow transients and with “relaxation strain”,  $\dot{\gamma}_0 t$ , after flow. These strain scalings have been verified in the model system PBLG/*m*-cresol from shear rates in Region II.<sup>1–3</sup> The stress relaxation and recoil occur on similar time scales and are usually complete before  $\dot{\gamma}_0 t \approx 100$ , with the absolute value depending on concentration and molecular weight. In addition to the stress relaxation, but at longer time scales, the elastic modulus  $|G^*|$  evolves after flow cessation.<sup>4</sup> The modulus measured after flow decreases, a behavior opposite to that seen in flexible polymer systems. This decrease in the moduli also scales with  $\dot{\gamma}_0 t$  but requires  $10^3$ – $10^4$  units to complete. Although the faster relaxation of the stress has been qualitatively explained in the context of the polydomain model, the slower relaxation of the moduli is poorly understood.

A study performed by Hongladarom and Burghardt<sup>5,6</sup> used a spectrographic birefringence technique to probe molecular alignment in the velocity–vorticity plane during and after flow in a series of PBG/*m*-cresol solutions. The measured birefringence was assumed to be proportional to the second moment of the rod orientation distribution  $\langle \mathbf{u}\mathbf{u} \rangle$ , where  $\mathbf{u}$  is a unit vector describing the orientation of a rodlike molecule. The authors observed that the birefringence under steady shear is only weakly dependent on shear rate at low rates and equivalent to about 53–63% of the monodomain value (see Figure 8 in ref 5). At higher shear rates, the birefringence exhibited a steep increase with shear rate, eventually reaching a high-shear plateau of 90% of the monodomain value. The observed increase in birefringence correlated with the rheological transition from positive to negative first normal stress difference, suggesting that the birefringence behavior is reflecting the transition from the low-shear-rate tumbling to the high-shear-rate flow-aligning regime.

After cessation of flow, the birefringence was observed, after an induction time, to increase rapidly to a long-time plateau value. Relaxations from shear rates in the range from 0.2 to 1.0 s<sup>−1</sup> scaled with  $\dot{\gamma}_0 t$ . This evolution of the birefringence correlated with a drop in the macroscopic elastic modulus; i.e., as the birefringence increased, the modulus decreased. As the modulus probes the degree of nematic alignment,<sup>7</sup> both observations are consistent with an increase in overall alignment after flow. The ratio of birefringence during shear to that at the end of the relaxation ranges from 53 to 63%, the ratio increasing with polymer concentration. This birefringence plateau value at very long times (values of  $\dot{\gamma}_0 t \geq 1000$ ) was observed to be comparable to the value measured for a monodomain formed via magnetic alignment.

The results obtained by Hongladarom and Burghardt<sup>6</sup> provide insight into the evolution of molecular alignment in flowing LCPs. Optical techniques are subject to several sources of ambiguity, such as surface effects, and the authors themselves point out several unexplained phenomena in their measurements. Our work presented here is a comparative study employing small-angle neutron scattering (SANS) to test and extend the birefringence results. We also introduce a simple and robust method to determine a quantitative order parameter from two-dimensional scattering patterns.

## Experimental Section

SANS experiments were performed on the 30 m beam line at NIST in Gaithersburg, MD. A quartz Couette cell with a 0.5 mm gap provided a controlled shear rate, with the beam perpendicular to the shear–velocity plane. Scattering experiments were performed at a sample-to-detector distance of 355 cm and wavelength of 5 Å  $\pm$  14.7%. Data were put on an absolute scale and corrected for instrument effects using standard procedures.<sup>8</sup>

A 17.4 wt % PBLG (Sigma lot no. 109 F5501) in d-DMF solution was prepared and allowed to equilibrate for 1 week before the experiments. Deuterated dimethylformamide (d-DMF) (Cambridge Isotope Laboratories) was used as received, but care was taken to avoid contamination by moisture, which causes aggregation in DMF solutions.<sup>9</sup> We assume that the only differences between the PBLG solutions in d-DMF and *m*-cresol will arise from the differences in solvent viscosity (the density of both solvents is  $\rho = 1.03$  g/cm<sup>3</sup>). The viscosity ratio is approximately 5, with *m*-cresol being the more viscous of the two, so the ratio of rotational diffusion coefficients is 1/5. Based on the established nondimensionalization of the shear rate with the rotational diffusivity,  $\dot{\gamma}/D_r$ , the shear rate in PBG/

\* To whom correspondence should be addressed; e-mail: wagner@che.udel.edu.

<sup>§</sup> Abstract published in *Advance ACS Abstracts*, February 15, 1996.

*m*-cresol solutions should be equivalent to a shear rate 5 times higher in PBG/d-DMF solutions (of equivalent polymer concentration and molecular weight).

The sample was brought to steady-state shear conditions at three different shear rates (0.4, 4, and 40 s<sup>-1</sup>), which are below the point where the first normal stress difference changes sign<sup>5</sup> and should be in the tumbling regime. The solution was presheared for at least 600 strain units at each shear rate before any data were collected. Behavior after cessation of shear was probed from each of these shear rates by collecting data in 10 min increments, the minimum time required to obtain data with a statistically low level of error.

### SANS Analysis

Extracting a quantitative measure of the molecular order in a solution from SANS data requires a scattering model. In this work, we have used a scattering model similar to that developed by Kalus *et al.*,<sup>10</sup> which we have employed previously to extract order parameters from magnetically aligned PBLG solutions.<sup>11</sup> Details of the assumptions of the model are explained in our earlier publication; here we begin with the following expression for the intensity:

$$I(\mathbf{q}) = C\phi V_p(\Delta\rho)^2 \langle F^2(\mathbf{q}) \rangle S_{\text{eff}}(q) \quad (1)$$

where  $C$  is a constant,  $\phi$  the volume fraction of rods,  $V_p$  the particle volume,  $(\Delta\rho)^2$  the scattering contrast, and  $S_{\text{eff}}(q)$  an effective structure factor that describes inter-rod interactions. The form factor is an average over the rod distribution  $f(\mathbf{u})$ , with  $\mathbf{u}$  the rod orientation, as

$$\langle F^2(\mathbf{q}) \rangle = \int f(\mathbf{u}) F^2(\mathbf{q}) d\mathbf{u} \quad (2)$$

For the system considered here, the limiting form factor for a long, thin rod is appropriate for the single particle scattering function  $F(\mathbf{q})$ .<sup>12</sup> Note that the form factor is much more complex than the simple expression used in calculating the intrinsic birefringence, for example. A spherical harmonic expansion of the form factor demonstrates that an infinite number of terms exist to couple to the rod distribution function. Thus, the projected scattering pattern contains information from *all* moments of the rod distribution function. It is possible, given an expression for the rod distribution function, to compare with a given scattering pattern and thus to extract the net order or alignment. In practice, this procedure is intractable, and if no additional information for the distribution function is known, is indeterminate. Thus, a more direct, but still accurate, measure of the order parameter is desired.

The measured scattered intensity is a projection of this scattered intensity onto a two-dimensional detector, and as such reduces the accessible information content. The scattering pattern from a nematic fluid can be decomposed into separable functions of the magnitude of the scattering vector ( $|\mathbf{q}| = q$ ) and the planar angle,  $\phi$ , where  $\phi = 0$  is defined as the flow or alignment direction. By symmetry, the primary  $\phi$  dependence of a partially aligned sample is expected to be of the form  $\cos(2\phi)$ , with the potential for all higher, even multiples existing.

To isolate this dominant contribution to the asymmetry, we define an "alignment factor" as follows:

$$A_f(q) \equiv \frac{\int_0^{2\pi} I(q, \phi) \cos(2\phi) d\phi}{\int_0^{2\pi} I(q, \phi) d\phi} \quad (3)$$

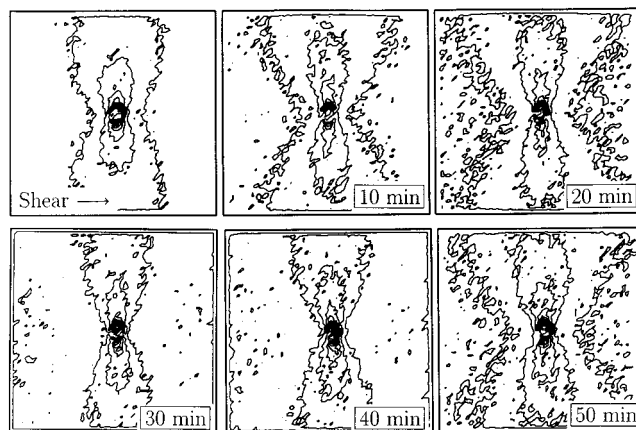


**Figure 1.**  $I(q, \phi)$  during and after shear at 4 s<sup>-1</sup>. These are projections in the velocity–vorticity plane. Data after shear cessation were taken in 10 min intervals.

In the limit of large  $qL$ , the structure factor will be inconsequential and the alignment factor will directly reflect the degree of molecular order *projected* onto the scattering plane. For an isotropic scattering pattern, the alignment factor will be zero at all values of  $q$ . In a system with the hourglass type pattern as seen in Figure 1,  $A_f(q)$  will be negative, decreasing to  $-1$  for a perfectly flow-aligned sample.

Both experimental data and model predictions can be reduced via this treatment and order parameter comparisons made. For example, the Maier–Saupe distribution about the alignment direction,  $\mathbf{x}$ ,

$$f(\mathbf{u}) = \frac{1}{Z} \exp(m(\mathbf{u} \cdot \mathbf{x})^2) \quad (4)$$

provides a convenient way to abstract a quantitative measure of an order parameter difference from the data for a *uniaxial* distribution. The scalar order parameter,  $S_m$ , is given by

$$S_m = \frac{3}{2} \langle (\mathbf{u} \cdot \mathbf{x})^2 \rangle - \frac{1}{3} \quad (5)$$

This order parameter is a measure of the distribution of molecules around the director and is directly comparable to birefringence measurements.  $S_m$  really corresponds to the  $S_{11} - S_{33}$  difference in order tensor components since the SANS experiment yields a net projection of the alignment of the macromolecules in the velocity–vorticity plane. Asymptotic analysis and numerical calculations demonstrate that  $A_f(q)$  becomes constant at  $qL \gg 1$ , which we will define as  $A_f^\infty$ . The numerical calculations also demonstrate that  $A_f^\infty = -S_m$ . This equality enables rapid and accurate determination of the order parameter from integration of the full scattering pattern. Note that this procedure is nearly equivalent to that employed by Picken<sup>13</sup> when applied to such a uniaxial distribution, except here the *full* scattering pattern is averaged and the wave vector dependence of the form factor properly accounted for. In fact, we used a technique similar to that of Picken in our earlier work on magnetically aligned PBLG.<sup>11</sup> Reanalysis of that data with the weighted averaging described in this work yields the same results but with higher accuracy. Further, our procedure can be applied to compare any theoretical model rapidly and efficiently to the data. Combining SANS patterns from different orthogonal projections would provide a method to de-

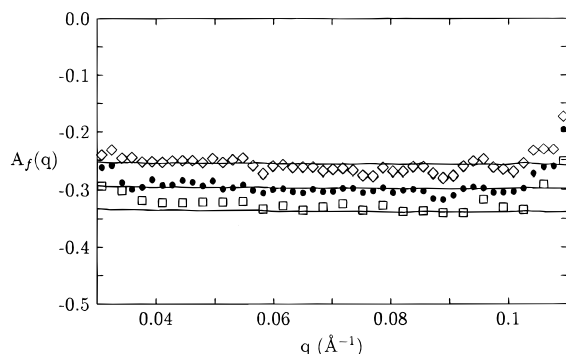


**Figure 2.** Alignment factors,  $A_f(q)$ , during steady shear at 0.4 (◇), 4 (●), and 40  $s^{-1}$  (□). Lines indicate the fit to a simple uniaxial model with  $S_m = 0.27, 0.30$ , and  $0.33$ .

termine the full second moment of a biaxial distribution, as typically observed under shear flow, for example.

In the following, we will determine alignment factors and report them as equivalent Maier–Saupe order parameters, for direct comparison to the previous birefringence measurements. Under flow, any biaxiality of the distribution function will distort this interpretation in a predictable manner.<sup>2,5,14</sup> As we expect the distribution function to be uniaxial upon relaxation, however, the interpretations should be accurate upon flow cessation.

## Results and Discussion

The anisotropy of these nematic solutions under shear and after cessation of shear is shown in the contour plots of the two-dimensional intensity profiles in Figure 1. This figure shows the pattern obtained under steady shear at  $\dot{\gamma} = 4 s^{-1}$ , the flow direction being horizontal in the figure, as well as the corresponding behavior upon flow cessation, with each pattern collected over a 10 min time period. During shear the scattering develops a high asymmetry, corresponding to a high degree of molecular alignment. From these images, however, it is difficult to visualize the degree of alignment and determine whether the relaxed structure is more or less aligned than the system under shear. Therefore, we employ a numerical integration routine to convert the two-dimensional intensity patterns to  $A_f(q)$  according to eq 3.

As observed in Figure 2, the steady shear alignment is nearly constant with shear rate. A similar, gradual increase with shear rate is reported in the previous birefringence study.<sup>5</sup> Picken also reported a nearly constant degree of alignment at similar shear rates for lyotropic aramid solutions based on an analysis of SAXS patterns.<sup>13</sup>

Figure 3 shows  $A_f(q)$  during shear and at various times during relaxation after cessation of shear. Note that most of the change in the overall alignment occurs during the first 10 min after cessation of shear. This is true of all three shear rates studied. Upon cessation of shear, the alignment increases, and in the case of the 4  $s^{-1}$  data, stays fixed at this higher level of alignment. A slight decrease in alignment is noted at 50 min, but it is not as significant as the initial increase after flow. The lines in Figure 3 correspond to the model prediction with order parameters of 0.30 and 0.52, as labeled. All of the  $A_f(q)$  measured asymptote at values of  $q > 0.07 \text{ Å}^{-1}$ ; so these values are reported as the macroscopic alignment factors,  $A_f^\infty$ . At lower  $q$ , the data and model lines do not agree due to the influence of interrod correlations.<sup>11</sup>

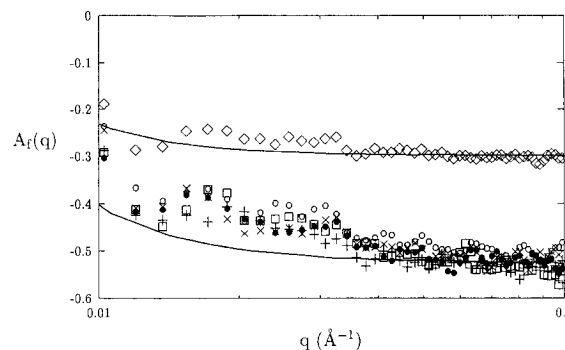


**Figure 3.** Alignment factors during and after shear at 4.0  $s^{-1}$ . Symbols are as follows: during shear (◇), 10 min (●), 20 min (+), 30 min (□), 40 min (×), and 50 min (○) after cessation of shear. The lines are the results of the model corresponding to values of 0.30 and 0.52 for the measured order parameter.

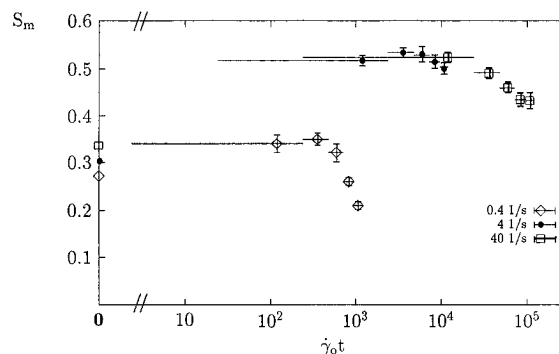


**Figure 4.** Effect of flow on the overall measured order parameter,  $S_m$ , given as  $-A_f^\infty$ . The vertical error bars are due to scatter in the  $A_f(q)$ , while the horizontal error bars arise from the fact that data were collected over 10 min intervals.

The results for all of our data, plotted as the order parameter  $S_m$ , where  $S_m = -A_f^\infty$ , are shown in Figure 4. Points on the left axis indicate the order parameter measured under shear. Focusing on the data for 4  $s^{-1}$  (●), the initial data taken upon flow cessation is an average over the first 2400 relaxation strain units (10 min), which corresponds to most of the transient relaxation of the birefringence as seen in the work of Hongladarom and Burghardt.<sup>6</sup> For the second pattern and beyond, the order parameter is constant with a value of  $0.53 \pm 0.02$ , as compared to the value under shear of  $0.30 \pm 0.01$ . The ratio of these two is 57%, which is consistent with the ratio of birefringences seen by Hongladarom and Burghardt. This is true also of the 40  $s^{-1}$  data, which rise from  $0.33 \pm 0.01$  to  $0.52 \pm 0.01$ , a ratio of 61%. Note that the lowest shear rate probed shows quantitatively different behavior. As this dimensionless shear rate is below that probed by Hongladarom and Burghardt, we will restrict the comparison to data taken in the same range of dimensionless shear rates.

To compare our results directly to those of Hongladarom and Burghardt, the measurements from both studies are tabulated in Table 1. Ratios are employed because Hongladarom and Burghardt reported birefringence in absolute units while we directly determine an order parameter. Our molecular weight and concentrations are slightly different than those used in the birefringence study, but, as shown in the table, our solution falls between theirs and both absolute and normalized concentration. Concentrations are given both in g/mL and normalized with respect to  $c^*$ , with  $c^*$  assumed to be 11 wt % for all molecular weights

**Table 1. Birefringence (\*, Ref 6) and SANS (†, This Work) Results, Provided as Ratios for Comparison between Techniques<sup>a</sup>**

solution	MW	<i>c</i> (g/mL)	<i>c/c*</i>	ratios (%)		
				<i>low</i> $\dot{\gamma}$ /relaxed	<i>low</i> $\dot{\gamma}$ /monodomain	relaxed/monodomain
13.5% PBG (*)	301 000	0.143	1.23	53	53	100
17.0% PBLG (†)	236 000	0.185	1.55	59 ± 3	58 ± 3	98
20.0% PBG (*)	301 000	0.214	1.80	63	63	100

<sup>a</sup> Monodomain values for the 17 wt % system were estimated from work on a magnetically aligned system.<sup>11</sup>

above 200 000. The comparison demonstrates the agreement between the two techniques, with our results for the increase in alignment after flow cessation (*low*  $\dot{\gamma}$ /relaxed) following the trend with concentration shown via birefringence. Our results show a slight shear rate dependence of the order parameter, as indicated by the  $\pm 3\%$  in the table.

In the birefringence study, the birefringence of a monodomain was measured and used to gauge the overall order in the system. For comparison, we use the value  $A_f^\infty = -0.54$  as measured in our previous work for a 16 wt % solution of PBLG aligned in a 1 T magnetic field for 8 h as a "monodomain" value. Again, the agreement with the trends seen in birefringence are excellent. One complication arises in that the order parameter expected for a monodomain should be much higher ( $S \approx 0.80$ ) than we measured in our magnetically aligned solution.

At very high levels of relaxation strain, corresponding to times of 50 min or more, the order parameter begins to decrease. This correlates with observations of long-time increases in the modulus<sup>3,4,15</sup> observed on similar, but not identical, solutions. Hongladarom and Burghardt did not report birefringence measurements at these large times. We cannot rule out the possibility that this decrease is surface-driven reorientation as its onset occurs *roughly* at the same time of relaxation. Estimates of the characteristic nematic reorientation time for this sample thickness indicate times an order of magnitude greater than observed here, but the quantities involved are only approximately known.

As noted, the low-shear-rate data show markedly different behavior as the order parameter remains nearly constant upon flow cessation, rising only a small amount during the first 20 min of relaxation ( $\dot{\gamma}_0 t = 480$ ), but then decreases significantly. Relaxation behavior from shear rates this low ( $0.4 \text{ s}^{-1}$  is comparable to  $0.08 \text{ s}^{-1}$  in *m*-cresol) were not probed by Hongladarom and Burghardt. It should be noted that at 50 min after cessation of flow, the overall orientation is *lower* than that measured under flow, which indicates qualitatively different behavior. The reason for this difference in behavior is unexplained at present but is currently under investigation.<sup>16</sup>

## Conclusions

The alignment factor technique presented here provides a robust method for quantitatively extracting the

order parameter from two-dimensional scattering images. Our SANS measurements support an earlier birefringence study<sup>6</sup> in that we observe quantitatively similar degrees of molecular orientation for Region II flows and comparable increases in overall order upon flow cessation in the same region of dimensionless shear rate. However, our work shows some additional features not probed in the previous work: at very long times or  $\dot{\gamma}_0 t > 10^4$ , we observe a decrease in order that might correlate with the increase observed in the elastic modulus; furthermore, anomalies are seen for relaxations from a lower shear rate than previously explored, which are not fully understood as of yet.

**Acknowledgment.** Funding for this work was provided by the NSF (Grant CTS-9158146) and DuPont Polymer Technology. This material is based upon activities supported by the National Science Foundation under Agreement No. DMR-9122444 at NIST. We thank W. R. Burghardt, K. Hongladarom, and B. Hammouda for useful discussions.

## References and Notes

- Moldenaers, P.; Yanase, H.; Mewis, J. J. *Rheol.* **1991**, *35*, 1681–1699.
- Larson, R. G.; Doi, M. *J. Rheol.* **1991**, *35*, 539–563.
- Walker, L. M.; Wagner, N. J.; Larson, R. G.; Mirau, P. A.; Moldenaers, P. *J. Rheol.* **1995**, *39*, 925–952.
- Moldenaers, P.; Mewis, J. J. *Rheol.* **1986**, *30*, 567–584.
- Hongladarom, K.; Burghardt, W. R.; Baek, S.-G.; Cementwala, S.; Magda, J. J. *Macromolecules* **1993**, *26*, 772–784.
- Hongladarom, K.; Burghardt, W. R. *Macromolecules* **1993**, *26*, 785–794.
- Moldenaers, P.; Mewis, J. J. *Rheol.* **1993**, *37*, 367–380.
- Barker, J.; Krueger, S.; Hammouda, B. SANS Data Reduction and Imaging Software, Technical Report, National Institute of Standards and Technology, Cold Neutron Research Facility, 1993.
- Block, H. *PBLG and Other Glutamic Acid Forming Polymers*; Gordon and Breach: New York, 1983.
- Kalus, J.; Hoffmann, H.; Ibel, K. *Colloid Polym. Sci.* **1989**, *267*, 818–824.
- Wagner, N. J.; Walker, L. M. *Macromolecules* **1994**, *27*, 5979–5986.
- van de Hulst, H. C. *Light Scattering by Small Particles*; Dover: New York, 1981.
- Picken, S. J.; Aerts, J.; Visser, R.; Northolt, M. G. *Macromolecules* **1990**, *23*, 3849–3854.
- Hongladarom, K.; Burghardt, W. R. *Macromolecules* **1994**, *27*, 483–489.
- Larson, R. G.; Mead, D. W. *J. Rheol.* **1989**, *33*, 1251–1281.
- Burghardt, W. B., *private communication*, 1995.

MA951127P